ISSN: 0369-8963

Tribological investigations on HfC reinforced AZ31 Magnesium Metal Matrix Composites

P. SATHISH KUMAR[1*], P. GOPAL[2], T. SENTHILKUMAR[3]

[1] Research Scholar, Department of Automobile Engineering, University College of Engineering, Anna University – BIT Campus, Tiruchirappalli – 620 024, Tamil Nadu, India, Email: sathishpauto@gmail.com, Cell: +91 9677887712*

[2]Assistant Professor, Department of Automobile Engineering, University College of Engineering, Anna University – BIT Campus, Tiruchirappalli – 620 024, Tamil Nadu, India, Email: pgopal@aubit.edu.in, Cell: +91 9443051196

[3]Professor, Department of Automobile Engineering, University College of Engineering, Anna University – BIT Campus, Tiruchirappalli – 620 024,Tamil Nadu, India, Email: kmtsenthil@gmail.com, Cell: +91 9443267846

Abstract

In this paper, an attempt was made to prepare Magnesium Metal Matrix Composites (MMCs) using AZ31 Mg as matrix material and hafnium carbide (HfC) as reinforcement material. AZ31-HfC Mg MMCs were prepared by using stir casting method using different HfC reinforcement percentages such as 5%, 10% & 15% by wt. Tensile tests and surface micro hardness tests on AZ31-HfC Mg MMCs were conducted. Yield strength & ultimate tensile strength & surface micro hardness of AZ31-HfC MMCs was found to increase up to 12%, 17% & 23% compared to base material AZ31 Mg alloy. Tribological studies were conducted using three sliding speeds (2 mm/s, 4 mm/s and 6 mm/s). Micro scratch tests were conducted on traction force and coefficient of abrasive friction variations. Pin on disc wear tests were conducted to study the wear mass loss of AZ31-HfC MMCs at different loading conditions, sliding rate and reinforcement percentage of HfC by wt. SEM analysis of wear tested specimens indicated voids, furrows, micro-cracks and wear debris.

Keywords: *AZ31, composites, hafnium carbide, tribology, wear.*

1. Introduction

Metal Matrix Composites (MMCs) are preferred in manufacturing sectors as they exhibit enhanced properties without compromising their parent alloy characteristics (Guo et al. 2011). MMCs exhibit enhanced corrosion and wear resistance than their parent alloys (Venkatesh & Rao 2018). Magnesium is a light weight material. Mg and its alloys are used in structural, manufacturing, automotive and electrical sectors as they exhibit enhanced thermal conductivity, high strength and low density (Liu et al. 2019. A lot of advantages were observed on reinforcing Mg alloys with different types of reinforcements. Improvement in tribological properties (higher wear resistance) was observed on reinforcing Mg alloy with B_4C reinforcements (Paidar et al. 2021). Nano bioceramic (nano bio-glass) reinforced Mg MMCs exhibits better mechanical properties and corrosion resistance (Khodaei et al. 2019).

. In this investigation, an attempt has been made to evaluate the tribological characteristics of HfC reinforced AZ 31 Mg MMCs.

 https://doi.org/10.37896/pd91.3/9133

ISSN: 0369-8963

2. Materials and methods

In this investigation, AZ31 Magnesium alloy was used as the matrix material for preparing Mg MMCs. Rolled AZ31 Mg alloy material was procured from M/s. Technolloy Inc, Mumbai. The procured AZ31 Mg material was cut into small pieces after thoroughly cleaning it with phenol to remove unwanted dust and dirt. AZ31 Mg was tested using spark spectrometer for identification of its chemical composition (Hussain et al. 2011). Cleaned AZ31 Mg sample was placed in spark spectrometer and by igniting sparks at different regions; its elemental composition was identified. The chemical composition of AZ31 Mg in wt. percentage is shown in Table 1.

Table 1. Chemical composition of AZ31 Mg in wt. percentage

Alloy	Al	Zn	Mn	Si	Cu	Ca	Fe	Ni	Mg
AZ31 Mg	2.3	1.1	0.16	0.06	0.03	0.034	0.041	0.039	Bal

Hafnium Carbide (HfC) was used as reinforcement material. 99.9% pure HfC powder was procured from M/s. Nano Research Elements, New Delhi. Stir casting process was used for preparing AZ31-HfC Mg MMCs (Kumar et al. 2018). Measured quantities of AZ31 Mg alloy pieces and HfC powder was placed in steel crucible of the furnace and heated. For melting Mg alloy, the temperature of the furnace was increased to 750°C (Behnamian et al. 2022). The mixture was retained at that temperature till it became semi solid. To evenly distribute HfC in Mg (having wide density difference), stirring was done at 400 rpm for 30 minutes (Huang et al. 2021). After mixing HfC in Mg matrix, the furnace temperature was increased to 1000°C (Lotfpour et al 2021). At 1000°C, the mixture was retained for 15 minutes. Then, for lowering the density of molten Mg matrix, temperature of the furnace was decreased to 700°C and stirring of the mix was started at 200 rpm (Wang & Rong 2021). After stirring the mixture for 20 minutes, it was poured into cylindrical moulds for solidification. The cylindrical moulds were pre-heated to 400°C, for preventing directional solidification (Kumar & Murugan 2012). For minimizing oxidation and sputtering, the entire casting process was done in inert gas (argon) atmosphere (Zhang et al. 2022).

Three sets of HfC reinforced AZ31 Mg MMCs were prepared by increasing HfC percentage. AZ31 Mg MMC sets were prepared using 5%, 10% & 15% HfC reinforcement by weight. For identifying the effect of HfC addition, one set was cast without HfC reinforcement (0% by weight). For identification, the as cast HfC reinforced Mg MMCs were designated as shown in Table 2.

 https://doi.org/10.37896/pd91.3/9133

ISSN: 0369-8963

Table 2 – Designation of the as-cast HfC reinforced Mg MMCs

S No.	AZ31 Mg (wt.%)	HfC (wt. %)	Designation
1	100	0	AZ31-BM
2	95	5	AZ31-05HfC
3	90	10	AZ31-10HfC
4	85	15	AZ31-15HfC

The tensile characteristics of AZ31-HfC Mg MMCs were evaluated using an electro-pneumatically controlled Universal Testing Machine (Make – INSTRON). As per ASTM E 08 standards, tensile test samples were prepared from AZ31-HfC Mg MMCs (Lv et al. 2019). By using an incremental load of 1.5 kgf/min, the samples were subjected to tensile loading till fracture.

Stress strain graphs were plotted and the corresponding changes in Yield Strength (YS), Ultimate Tensile Strength (UTS) and percentage of elongation of HfC reinforced Mg MMCs were calculated. Variations in the surface micro hardness of AZ31-HfC Mg MMCs were calculated using Vickers micro hardness testing equipment (Make – EQUITOP). As per AZTM E 384 standards, micro hardness testing was conducted on AZ31-HfC Mg MMCs (Srivastava et al. 2019). A load of 20 kgf was placed on the samples for 15 seconds and the indentation was evaluated for calculating the micro hardness. The compounds and elements formed in AZ31-HfC Mg MMCs during stir casting process were identified using X-Ray Diffraction Spectroscopy (Make-RIGAKU). XRD analysis was done using a copper target with step size of 0.002, within 20° to 80° two theta (2θ) (Feng et al. 2020). For conducting microstructural investigations on AZ31-HfC Mg MMCs, the specimens were prepared by using standard metallurgical procedures (Gao et al. 2018). The surface of the specimens was initially polished using 4 different grades of emery sheet. After emery polishing, it was cleaned using phenol. Then, the specimens were subjected to fine polishing using diamond grit paste coated disc polishing equipment (Lei et al. 2010).

Scanning Electron Microscopic (SEM) studies were done using Nitrogen chamber fitted Scanning Electron Microscope (Make –Leads). SEM images were evaluated to identify the modifications in the surface characteristics of AZ31-HfC Mg MMCs.

For evaluating the surface integrity of AZ31-HfC Mg MMCs, micro scratch tests were conducted. As per ASTM C-1624 standards, micro scratch testing was conducted (Farnoush et al. 2015). Micro scratch test specimens were polished using emery before subjecting them to tests. 5 scratches were done per test sample with starting and ending load of 20 N, 15 mm stroke length, 100 µm/s scratching velocity and 2 mm scratching offset. By conducting micro scratch

 https://doi.org/10.37896/pd91.3/9133

ISSN: 0369-8963

tests, the traction force was calculated. By dividing traction force with normal load, the coefficient of abrasive friction was conducted (Ghosh et al. 2008).

Tribo wear tests on AZ31-HfC Mg MMCs were conducted using pin on disc tribo wear testing equipment (Make-DUCOM). As per ASTM G133 standards, AZ31-HfC Mg MMC pins were prepared (Arnaud et al. 2021). EN31 steel plate was used as testing disc, with a track diameter of 80 mm. The load on pins was varied from 20N to 80N and the wear experiments were conducted without lubrication. The duration of the test was between 4 to 8 minutes depending upon sliding speed. Three sliding speeds such as 2 m/s, 4 m/s and 6 m/s were used in the experiments.

The variations in specific wear rate and coefficient of friction was identified on increasing HfC reinforcements in AZ31 Mg MMCs. Wear mass loss was calculated by measuring the weight of the pins before and after wear experiments. After wear testing, the specimens were subjected to microstructural analysis using SEM. The surface modifications in MMC surfaces were identified.

3. Results & Discussion

3.1 Tensile test results

The Yield Strength (YS) and Ultimate Tensile Strength (UTS) of AZ31-BM were recorded as 173 MPa and 246 MPa respectively. On adding 5% HfC, YS and UTS of AZ31-05HfC increased by 10.4% and 8.13%, compared to the base material. On increasing HfC reinforcement to 10% by wt., YS and UTS of AZ31-10HfC increased by 13.8% and 15.04%, compared to the base material. Increase in tensile characteristics was observed on increasing the HfC reinforcement till 10% by wt. On increasing HfC reinforcement up to 15% by weight, YS and UTS of AZ31-15HfC reduced by 1.54% and 4.4% compared to AZ31-10 HfC. The tensile test results of AZ31-HfC Mg MMCs are shown in Table 3.

Table 3. Tensile test results of AZ31-HfC Mg MMCs

Composite	Yield Strength (YS) (MPa)	Ultimate Tensile Strength (UTS) (MPa)	Elongation %	Micro hardness (HV)
AZ31-BM	173 ± 3	246 ± 3	13.1 ± 0.4	57 ± 3.2
AZ31-05HfC	191 ± 2	266 ± 2	08.6 ± 0.5	68 ± 0.71
AZ31-10HfC	197 ± 3	283 ± 2	06.4 ± 0.5	71 ± 0.58
AZ31-15HfC	194 ± 4	271 ± 3	05.2 ± 0.3	84 ± 1.12

The stress - strain graphs of AZ31- BM and the three HfC reinforced AZ31 Mg MMCs are shown in Fig. 1.

 https://doi.org/10.37896/pd91.3/9133

ISSN: 0369-8963

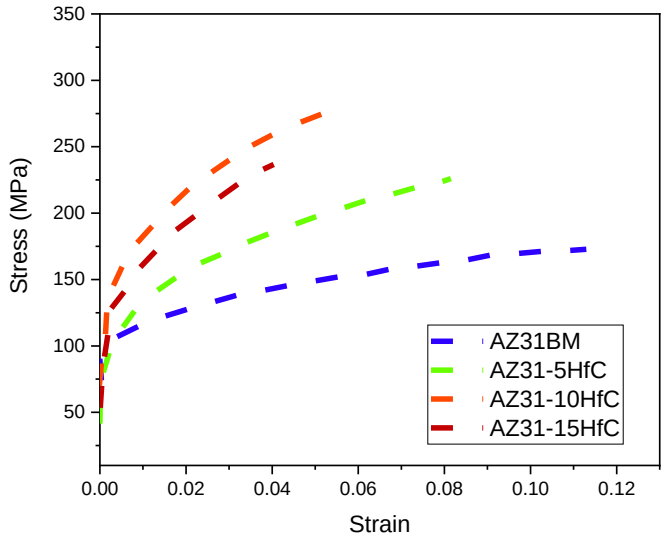

Fig. 1. Stress Strain graphs of AZ31-HfC MMCs

The surface micro hardness variations of HfC reinforced AZ31-Mg MMCs are shown in Fig. 2.

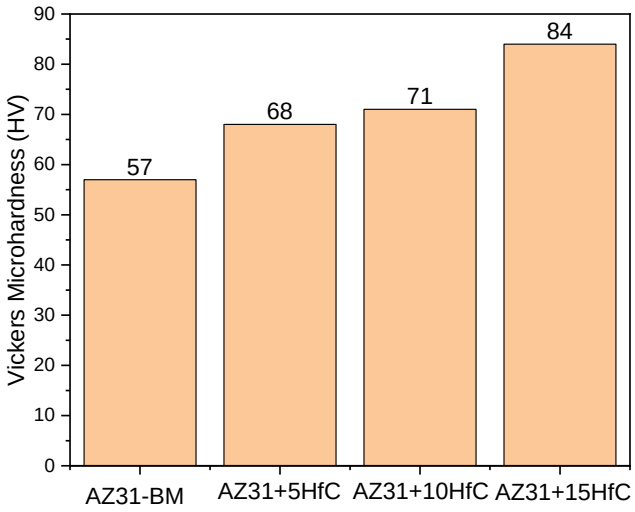

Fig. 2. Micro hardness variation of HfC reinforced AZ31 Mg MMCs

AZ31-BM without HfC addition shoed the micro hardness value as 57 HV. On addition of HfC reinforcements, a consistent increase in micro hardness of AZ31-HfC Mg MMCs was observed. The micro-hardness of AZ31-5HfC increased by 19.2%, compared to AZ31-BM. Similarly, the micro hardness of AZ31-10HfC and AZ31-15HfC increased 24.5% and 47.4%, compared to the base material.

 https://doi.org/10.37896/pd91.3/9133

ISSN: 0369-8963

In micro scratch experiments, the variations in traction force with HfC reinforcements are shown in Fig. 3a. Scratch resistance increases on increasing reinforcement percentage in MMCs (Pramanik 2016). During micro scratch experiments, heating in the scratch region changes residual depth causing visco-elastic recovery (Karimzadeh & Ayatollahi 2014). Increase in HfC reinforcements causes a reduction in penetration depth (scratch depth/ microns) during micro scratch experiments. Increase in HfC reinforcement causes a change in traction force. A consistent increase in traction force was observed on increasing the HfC reinforcement percentage, due to a reduction in visco elastic healing.

Variations in coefficient of abrasive friction with increase in HfC reinforcements are shown in Fig. 3b. Strong visco elastic behavior of the MMCs during micro scratch tests influences the coefficient of abrasive friction. Reinforcement addition in MMCs influences pure elastic recovery, inhibiting scratch healing (Dong et al. 2015). Bond reformation occurs between HfC reinforcement particles and Mg matrix, after removal of the force on the surface imposed by the scratching tip. Therefore, coefficient of abrasive friction was found to increase on adding HfC reinforcements.

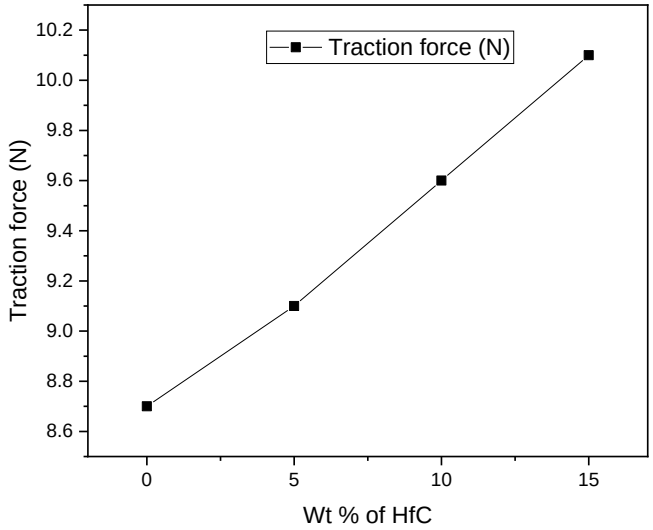

(a)

 https://doi.org/10.37896/pd91.3/9133

ISSN: 0369-8963

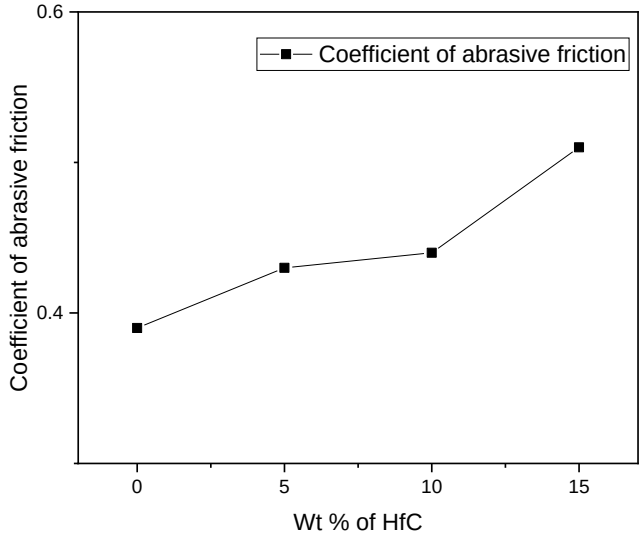

(b)

Fig.3.(a). Traction force variations on increasing HfC reinforcement percentage in AZ31-HfC MMCs, (b). Coefficient of abrasive friction variations on increasing HfC reinforcement in AZ31-HfC MMCs

Variations in specific wear rate at sliding speed of 2mm/s, 4 mm/s & 6 mm/s are shown in Fig. 4a, Fig. 4b & Fig. 4c, respectively. At low sliding speed of 2 mm/s, entire specific wear rate of all the combinations lies between 0.85 x 10^{-6} mm^3/Nm and 0.45 x 10^{-6} mm^3/Nm (Fig. 4a). For HfC reinforced Mg MMCs, at lower loads, the curves are wide and at higher loads, the curves are shallower. HfC reinforcement in Mg provides significant protection against wear. Under similar tribo wear testing conditions, reinforcement addition in MMCs causes its melt viscosity to increase (Lloyd 1994). Reduction in specific wear rate is observed on increasing load. For all combinations of HfC reinforced AZ31 Mg MMCs, reduction in specific wear rate is observed. On increasing HfC reinforcement to 10% by weight, specific wear rate reduces. On increasing HfC reinforcements beyond 10%, specific wear rate increases.

 https://doi.org/10.37896/pd91.3/9133

ISSN: 0369-8963

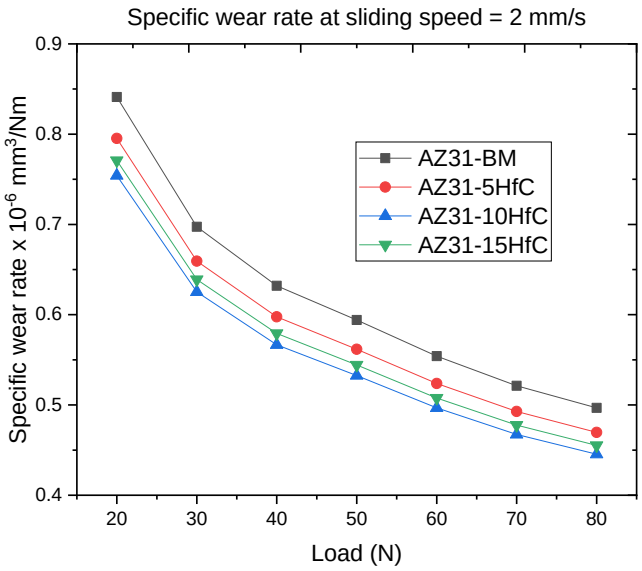

a) Specific wear rate with load at sliding speed 2 mm/s

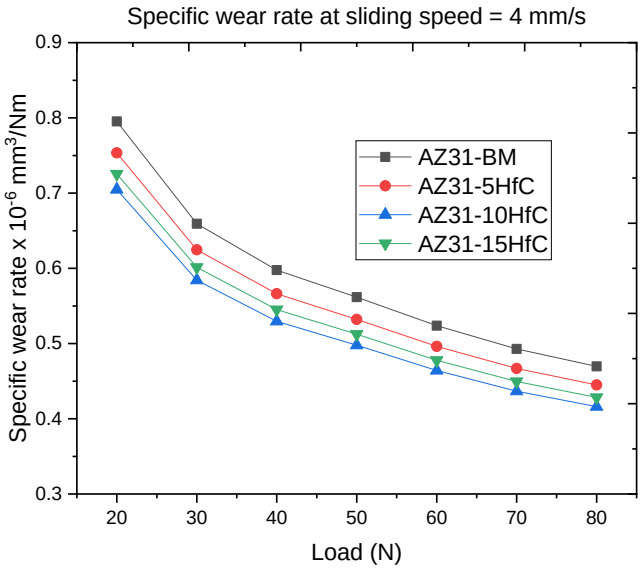

b) Specific wear rate with load at sliding speed 4 mm/s

https://doi.org/10.37896/pd91.3/9133

ISSN: 0369-8963

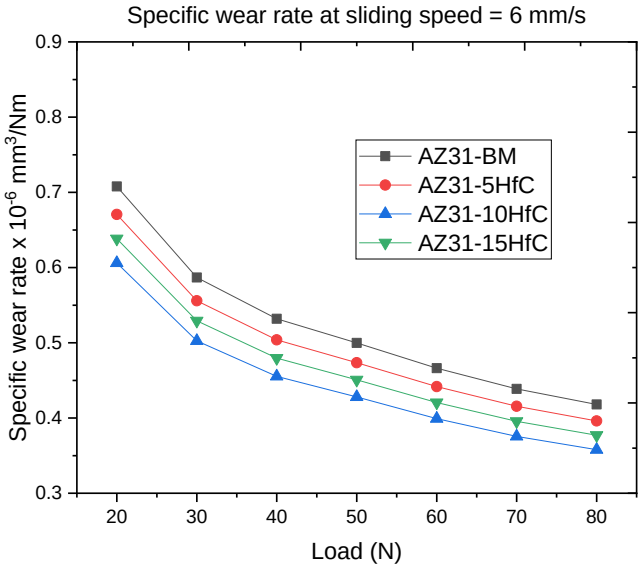

c) Specific wear rate with load at sliding speed 6 mm/s

Fig. 4. Variations in specific wear rate at sliding speed of a). 2mm/s, b) 4mm/s, c) 6mm/s.

At sliding speed of 4 mm/s (Fig. 4b), entire specific wear rate of all the combinations are between 0.8 x 10^{-6} mm^3/Nm and 0.4 x 10^{-6} mm^3/Nm. Increase in sliding speed results in reduction in specific wear rate for all combinations at all loads. Tribo wear causes detrimental changes to the surface of the test specimens. HfC particles increases the friction resistance behavior of MMCs, during dry sliding wear tests against the tribo wear disk. HfC reinforcements increase the beneficial effect such as specific wear reduction (Adesina et al. 2019). Doubling the contents of HfC micro particles (from 5% to 10% y wt.) provides better wear resistance. Oscillation of specific wear rate occurs on increasing the HfC reinforcement from 5% to 15% (10% HfC being the middle). For all HfC reinforced Mg MMCs and base material, at same contact pressure, increase in sliding speed from 2 mm/s to 6 mm/s cause a reduction in specific wear rate. At sliding speed of 6 mm/s, (Fig. 4c), lower specific wear rate for 5% HfC and 10% HfC reinforced Mg MMCs are observed. These are due to the protection of MMC surface against scratching and wear owing to HfC particles. Smoothening of generally irregular surfaces by reinforcements reduces wear (Jia & Gu 2014).

Variations in coefficient of friction upon increasing Load at sliding speed of 2mm/s, 4mm/s & 6mm/s is shown in Fig. 5a, Fig. 5b. & Fig. 5c. Increase in coefficient of friction was observed upon increasing load. Increase in HfC reinforcement till 10% by weight, decreased coefficient of friction. Further, on increasing HfC reinforcements caused decrease in coefficient of friction. At sliding speed of 2 mm/s (Fig. 5a), the strong bond between HfC and Mg matrix helps to maintain the broken pieces within the composite surface, preventing the formation of third phase particles and reducing wear. From 20 N to 80 N load, the variations in coefficient of

 https://doi.org/10.37896/pd91.3/9133

ISSN: 0369-8963

friction were between 0.22 and 0.14, for all HfC combinations. Coefficient of friction decreases with increase in HfC percentage.

High performance composite with optimum wear resistance is observed at 10% HfC reinforcement (Fig. 5b). At 4 mm/s sliding speed, for all samples, the entire coefficient of friction variation graph shifted lower, between 0.21 and 0.135. Wear resistance increases and coefficient of friction reduces for all loading conditions, on increasing HfC reinforcements. HfC reinforcements exhibit excellent wear and friction performance.

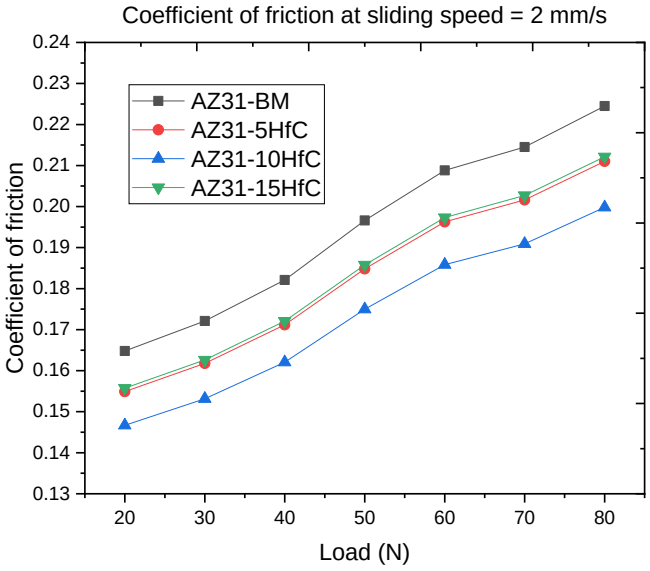

a) Coefficient of friction with load at 2mm/s

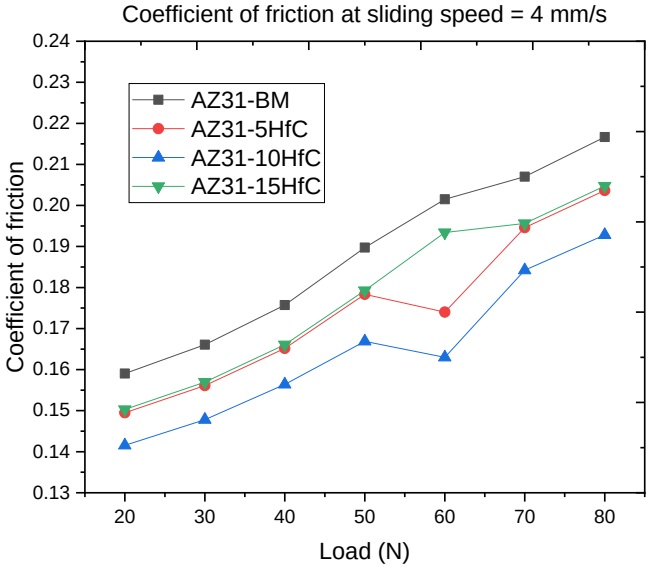

 https://doi.org/10.37896/pd91.3/9133

ISSN: 0369-8963

b) Coefficient of friction with load at 4 mm/s

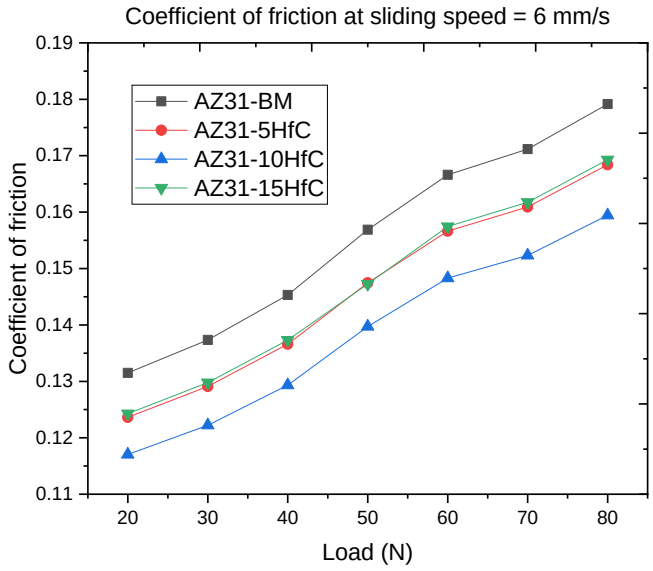

c) Coefficient of friction with load at 6mm/s

Fig.5. Variations in coefficient of friction with load at sliding speed a) 2 mm/s, b) 4 mm/s, c) 6 mm/s.

At sliding speed of 6 mm/s, the variations in coefficient of friction shifted lower, between 0.175 and 0.115, for all reinforcement combinations of Mg MMCs (Fig. 5c). The tribological characteristics of Mg MMCs get affected due to the interfacial bonding between the matrix and reinforcement material (Cai et al. 2016). Coefficient of friction values of HfC reinforced Mg MMCs are significantly lower than un-reinforced Mg base alloy. Unreinforced Mg alloys had minimal asperities. Subjecting them to wear tests resulted in ploughing action, increasing the friction coefficient. Decrease in coefficient of friction with increase in sliding velocity was attributed to the change in shear rate (Muratov et al. 1998).

Variations in mass loss upon increasing Load at sliding speed of 2mm/s, 4mm/s & 6mm/s is shown in Fig. 6a, Fig. 6b. & Fig. 6c. For all reinforcement combinations, increase in wear mass loss was observed upon increasing load. On increasing HfC reinforcements till 10% by wt., reduction in wear mass loss is observed. Increasing HfC reinforcement beyond 10% by wt., results in increased wear loss. At 2 mm/s sliding speed, the range of wear mass loss for all the combinations are found to be between 0.41 g to 0.25 g (Fig. 6a). Reduction in the coefficient of friction of the Mg MMCs improved its anti frictional behavior. This enhances lubricating effect

 https://doi.org/10.37896/pd91.3/9133

ISSN: 0369-8963

of the particles by forming an oxide film (Jerome et al. 2010), resulting in reduced wear mass loss. On increasing the loads in tribological experiments, removal of oxide films results in higher wear mass loss. Even though the mechanical characteristics of the Mg MMCs are enhanced by using HfC reinforcements, there is a drawback from the abrasiveness of these hard HfC particles. These particles cause a high friction coefficient in the contact region above a certain load. This causes increase in wear mass loss for 15% HfC reinforced Mg MMCs than 10% HfC reinforced Mg MMCs.

At sliding rate of 4 mm/s (Fig. 6b), the overall wear mass loss increased (between 0.44 g to 0.27 g), compared to the wear mass losses at sliding rate of 2 mm/s. On increasing the normal load applied in tribological experiments, an oxide layer forms on the surfaces due to increase in surface temperature (Komori & Umehara 2015). This oxide layer imparts a self lubrication effect and reduces friction between the tribo wear surfaces (Berman et al. 2013). On increasing the sliding velocity from 2 mm/s to 4 mm/s, the coefficient of friction reduces on increasing HfC reinforcements. The area of contact increases with respect to nominal area of contact on increasing the load on the test pin. This increased the frictional force between the sliding surfaces.

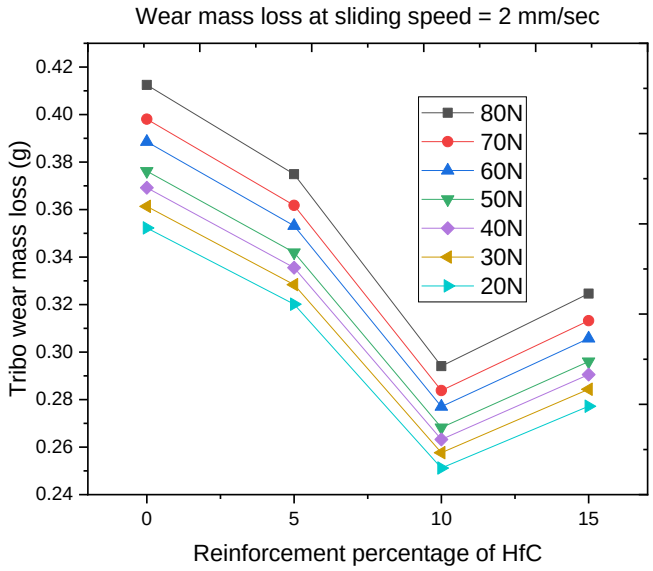

(a)

https://doi.org/10.37896/pd91.3/9133

ISSN: 0369-8963

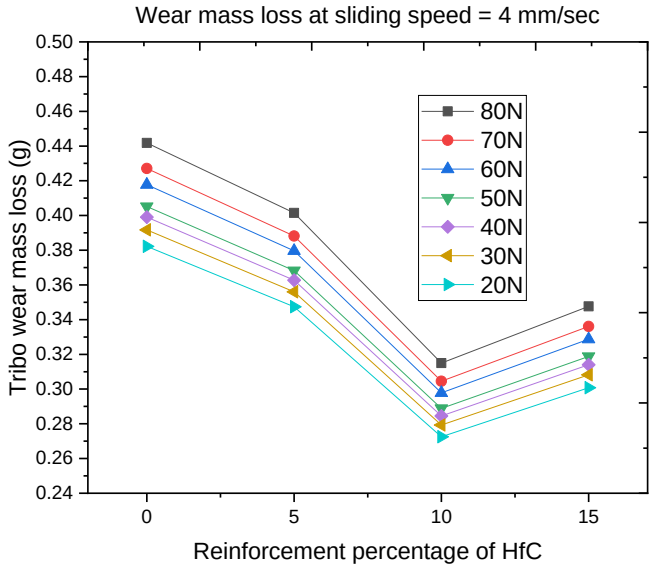

(b)

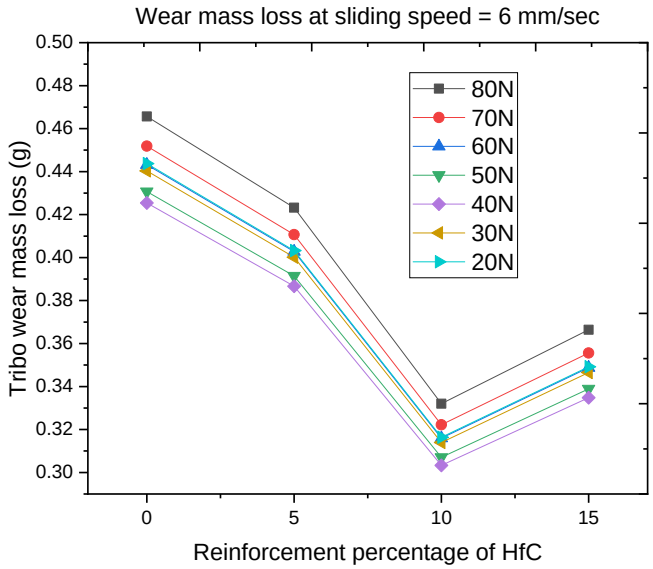

(c)

Fig. 6. Variations in mass loss with loads at sliding speed (a) 2 mm/s, (b) 4 mm/s, (c) 6 mm/s

On increasing the sliding speed to 6 mm/s, the overall wear mass loss for all combinations increased (between 0.47 g to 0.31 g) (Fig. 6c). Plastic deformation occurs at the asperities (tribo wear surfaces) until the actual contact area increases sufficiently for supporting the applied load (Saeidi et al. 2017). When a soft metal matrix composite (such as Mg MMC)

 https://doi.org/10.37896/pd91.3/9133

ISSN: 0369-8963

slides against hard disk material without liquid or solid lubrication, the softer one abrades, flows or adheres to the harder material, creating an interface of low shear strength (Erdemir 2005).

The SEM images of wear tested samples are shown in Fig. 7. Worn out flakes are observed in AZ31-BM along wear direction (Fig. 7a). When Mg surface slides with the disc under normal load, deformation occurs. Ploughing and wear occurs due to the formation of local pressure at the asperities. Strength of Mg MMCs are less at low shear strain rates, resulting in higher actual area of contact and higher coefficient of friction under dry wear conditions (Sumer et al. 2008). During tribo wear tests, the local pressure at the asperities increases to a very high value. As it exceeds the material yield stress value, wear occurs.

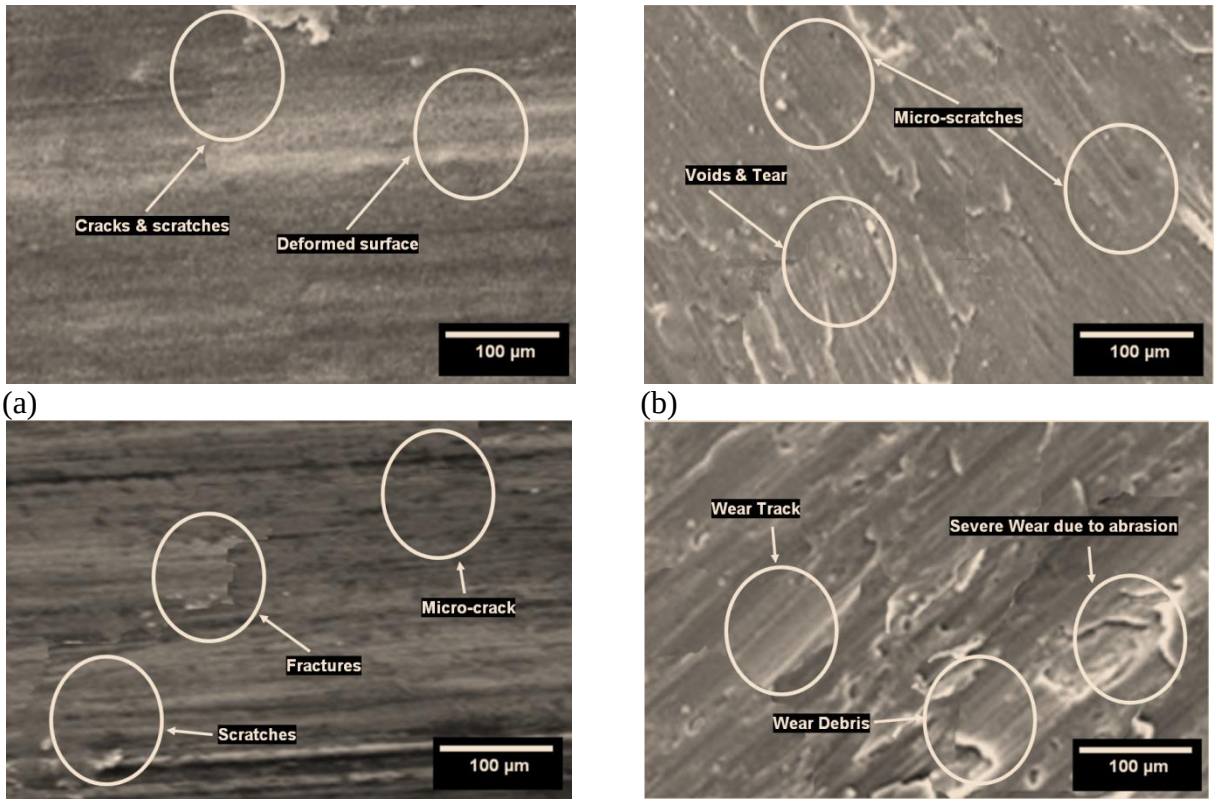

Fig. 7 SEM images of wear tested specimens (a) AZ31-BM, (b) AZ31-5HfC, AZ31-10HfC, AZ31-15HfC

Eruptions and tears are observed in AZ31-5HfC specimen (Fig. 7b). Wear occurs when HfC on the surface of the MMC gets removed due to MMC surface – wear disc interaction. Due to the stacked chemical structure of HfC micro particles, they act as solid lubricants. During wear tests, reinforcements in Mg surface exhibit weak inter layer bonding due to van der vaals

 https://doi.org/10.37896/pd91.3/9133

ISSN: 0369-8963

force (Ru et al. 2020). This provides least tangential resistance and enables low strength shearing in the interacting surfaces. During wear experiments, due to matrix-reinforcement interaction, powerful short range forces come into action. This causes formation of secure adhesive junctions at the actual area of contact (Poon & Sayles 1992). Micro-cracks and voids are formed due to the effect of hard disc surface sliding on softer Mg MMC surface.

Scratches and lines are observed in AZ31-10HfC samples (Fig.7c). Relative motion between MMC surface and wear disc causes shearing of adhered junction. The environment (disc) and the mating surface (Mg MMCs) undergo dynamic interaction which plays an important role during wear experiments (Schall et al. 2010). During sliding interaction, wear of surface due to abrasion causes crack formation. Frictional thrust and shear force increases with sliding due to clustering of HfC particles. Prolonged sliding accelerates wear rate, causing micro cracks, voids and micro-fractures on the surface.

Cracks perpendicular to wear direction is observed in AZ31-15HfC specimens (Fig.7.d). During wear experiments, abrasion causes bonding of the asperities on the surfaces of the contacting surfaces. Abrasive and erosive wear occurs when HfC particles trapped at the interface causes abrasive action against the surface in contact. Excessive HfC reinforcement's results in increased frictional force and actual contact surface area cause severe wear. Excessive rubbing results in formation of wear track and accumulated wear debris.

Conclusions

In this investigation, using stir casting, HfC reinforced AZ31 Mg MMCs were prepared and subjected to mechanical and tribological investigations.

1. Increase in yield strength and ultimate tensile strength was observed upon increasing HfC reinforcements up to 10% by weight. Excessive reinforcement (beyond 10% HfC) caused reduction in tensile characteristics of AZ31-HfC MMCs.

2. In micro scratch tests, traction force and coefficient of abrasive friction increased on increasing wt. percentage of HfC.

3. On conducting tribo wear tests, specific wear rate and coefficient of friction decreased upon increasing load. On increasing HfC reinforcements till 10% by weight, reduction in mass loss was observed. On increasing HfC reinforcements beyond 10% mass loss increased.

4. SEM analysis of wear tested specimens worn out flakes, eruptions, tears, scratches, lines and cracks perpendicular to wear direction.

 https://doi.org/10.37896/pd91.3/9133

References

Adesina, A.Y., Iqbal, Z., Al-Badour, F.A. and Gasem, Z.M., 2019. Mechanical and tribological characterization of AlCrN coated spark plasma sintered W–25% Re–Hfc composite material for FSW tool application. Journal of Materials Research and Technology, 8(1), pp.436-446. doi: https://doi.org/10.1016/j.jmrt.2018.04.004

Arnaud, P., Baydoun, S. and Fouvry, S., 2021. Modeling adhesive and abrasive wear phenomena in fretting interfaces: A multiphysics approach coupling friction energy, third body and contact oxygenation concepts. Tribology International, 161, p.107077. doi: https://doi.org/10.1016/j.triboint.2021.107077.

Behnamian, Y., Serate, D., Aghaie, E., Zahiri, R., Tolentino, Z., Niazi, H. and Mostafaei, A., 2022. Tribological behavior of ZK60 magnesium matrix composite reinforced by hybrid MWCNTs/B4C prepared by stir casting method. Tribology International, 165, p.107299. doi: https://doi.org/10.1016/j.triboint.2021.107299.

Berman, D., Erdemir, A. and Sumant, A.V., 2013. Few layer graphene to reduce wear and friction on sliding steel surfaces. Carbon, 54, pp.454-459. doi: https://doi.org/10.1016/j.carbon.2012.11.061.

Cai, M., Takagi, H., Nakagaito, A.N., Li, Y. and Waterhouse, G.I., 2016. Effect of alkali treatment on interfacial bonding in abaca fiber-reinforced composites. Composites Part A: Applied Science and Manufacturing, 90, pp.589-597. doi: https://doi.org/10.1016/j.compositesa.2016.08.025.

Cedillos-Barraza, O., Manara, D., Boboridis, K., Watkins, T., Grasso, S., Jayaseelan, D.D., Konings, R.J., Reece, M.J. and Lee, W.E., 2016. Investigating the highest melting temperature materials: A laser melting study of the TaC-HfC system. Scientific reports, 6(1), pp.1-11. doi: https://doi.org/10.1038/srep37962

Deng, K., Shi, J., Wang, C., Wang, X., Wu, Y., Nie, K. and Wu, K., 2012. Microstructure and strengthening mechanism of bimodal size particle reinforced magnesium matrix composite. Composites Part A: Applied Science and Manufacturing, 43(8), pp.1280-1284. doi: https://doi.org/10.1016/j.compositesa.2012.03.007

Dong, S., Zhou, J., Hui, D., Wang, Y. and Zhang, S., 2015. Size dependent strengthening mechanisms in carbon nanotube reinforced metal matrix composites. Composites Part A: Applied Science and Manufacturing, 68, pp.356-364. doi: https://doi.org/10.1016/j.compositesa.2014.10.018

Eivani, A.R., Tabatabaei, F., Khavandi, A.R., Tajabadi, M., Mehdizade, M., Jafarian, H.R. and Zhou, J., 2021. The effect of addition of hardystonite on the strength, ductility and corrosion

resistance of WE43 magnesium alloy. journal of materials research and technology, 13, pp.1855-1865. doi: https://doi.org/10.1016/j.jmrt.2021.05.027.

Erdemir, A., 2005. Review of engineered tribological interfaces for improved boundary lubrication. Tribology International, 38(3), pp.249-256. doi: https://doi.org/10.1016/j.triboint.2004.08.008

Farnoush, H., Mohandesi, J.A. and Çimenoğlu, H., 2015. Micro-scratch and corrosion behavior of functionally graded HA-TiO_2 nanostructured composite coatings fabricated by electrophoretic deposition. Journal of the mechanical behavior of biomedical materials, 46, pp.31-40. doi: https://doi.org/10.1016/j.jmbbm.2015.02.021.

Feng, S., Yang, Y., Wang, J., Wang, Y. and Zhou, X., 2020. Improved mechanical properties and fracture mechanism of C/C composites with salt treatment monitored by synchrotron-based in-situ tensile XRD. Composites Part B: Engineering, 199, p.108274. doi: https://doi.org/10.1016/j.compositesb.2020.108274.

Friend, C.M., 1987. The effect of matrix properties on reinforcement in short alumina fibre-aluminium metal matrix composites. Journal of materials science, 22(8), pp.3005-3010. doi: https://doi.org/10.1007/BF01086505

García-Rodríguez, S., Torres, B., Maroto, A., López, A.J., Otero, E. and Rams, J., 2017. Dry sliding wear behavior of globular AZ91 magnesium alloy and AZ91/SiCp composites. Wear, 390, pp.1-10. doi: https://doi.org/10.1016/j.wear.2017.06.010.

Gao, Y.Y., Qiu, F., Geng, R., Zhao, W.X., Yang, D.L., Zuo, R., Dong, B.X., Han, X. and Jiang, Q.C., 2018. Preparation and characterization of the Al-Cu-Mg-Si-Mn composites reinforced by different surface modified SiCp. Materials Characterization, 141, pp.156-162. doi: https://doi.org/10.1016/j.matchar.2018.04.049.

Ghosh, D., Subhash, G. and Orlovskaya, N., 2008. Measurement of scratch-induced residual stress within SiC grains in ZrB_2–SiC composite using micro-Raman spectroscopy. Acta Materialia, 56(18), pp.5345-5354. doi: https://doi.org/10.1016/j.actamat.2008.07.031.

Guo, S., Kang, G. and Zhang, J., 2011. Meso-mechanical constitutive model for ratchetting of particle-reinforced metal matrix composites. International Journal of Plasticity, 27(12), pp.1896-1915. doi: https://doi.org/10.1016/j.ijplas.2011.01.001

Guo, Y., Chen, J., Song, W., Shan, S., Ke, X. and Jiao, Z., 2021. Electronic, mechanical and thermodynamic properties of ZrC, HfC and their solid solutions studied by first-principles calculation. Solid State Communications, 338, p.114481., doi: https://doi.org/10.1016/j.ssc.2021.114481.

Huang, S.J., Subramani, M. and Chiang, C.C., 2021. Effect of hybrid reinforcement on microstructure and mechanical properties of AZ61 magnesium alloy processed by stir casting method. Composites Communications, 25, p. 100772. doi: https://doi.org/10.1016/j.coco.2021.100772.

Hussain, Z., Khan, K.M., Hussain, K., Hussain, S. and Perveen, S., 2011. Microwaves spark emission spectroscopy for the analysis of cations: A simple form of atomic emission spectroscopy. Chinese Chemical Letters, 22(9), pp.1084-1086., doi: https://doi.org/10.1016/j.cclet.2011.03.019.

Iqbal, Z., Saheb, N. and Shuaib, A.R., 2016. W-25% Re-HfC composite materials for Pin tool material applications: Synthesis and consolidation. Journal of Alloys and Compounds, 674, pp.189-199. doi: https://doi.org/10.1016/j.jallcom.2016.03.030

Jerome, S., Ravisankar, B., Mahato, P.K. and Natarajan, S., 2010. Synthesis and evaluation of mechanical and high temperature tribological properties of in-situ Al–TiC composites. Tribology International, 43(11), pp.2029-2036. doi: https://doi.org/10.1016/j.triboint.2010.05.007

Jia, Q. and Gu, D., 2014. Selective laser melting additive manufacturing of TiC/Inconel 718 bulk-form nanocomposites: Densification, microstructure, and performance. Journal of Materials Research, 29(17), pp.1960-1969. doi: oi:10.1557/jmr.2014.130

Karimzadeh, A. and Ayatollahi, M.R., 2014. Mechanical properties of biomaterials determined by nano-indentation and nano-scratch tests. In Nanomechanical Analysis of High Performance Materials (pp. 189-207). Springer, Dordrecht. doi: https://doi.org/10.1007/978-94-007-6919-9_10

Khan, M.M. and Nisar, M., 2022. Effect of in situ TiC reinforcement and applied load on the high-stress abrasive wear behaviour of zinc–aluminum alloy. Wear, 488, p.204082. doi: https://doi.org/10.1016/j.wear.2021.204082.

Khodaei, M., Nejatidanesh, F., Shirani, M.J., Valanezhad, A., Watanabe, I. and Savabi, O., 2019. The effect of the nano-bioglass reinforcement on magnesium based composite. Journal of the Mechanical Behavior of Biomedical Materials, 100, p.103396., doi: https://doi.org/10.1016/j.jmbbm.2019.103396.

Komori, K. and Umehara, N., 2015. Effect of surface morphology of diamond-like carbon coating on friction, wear behavior and tribo-chemical reactions under engine-oil lubricated condition. Tribology International, 84, pp.100-109. doi: https://doi.org/10.1016/j.triboint.2014.11.010

Kumar, A., Kumar, S. and Mukhopadhyay, N.K., 2018. Introduction to magnesium alloy processing technology and development of low-cost stir casting process for magnesium alloy and

its composites. Journal of magnesium and Alloys, 6(3), pp.245-254. doi: https://doi.org/10.1016/j.jma.2018.05.006.

Kumar, B.A. and Murugan, N., 2012. Metallurgical and mechanical characterization of stir cast AA6061-T6–AlNp composite. Materials & Design, 40, pp.52-58. doi: https://doi.org/10.1016/j.matdes.2012.03.038.

Lei, H., Bu, N., Chen, R., Hao, P., Neng, S., Tu, X. and Yuen, K., 2010. Chemical mechanical polishing of hard disk substrate with α-alumina-g-polystyrene sulfonic acid composite abrasive. Thin Solid Films, 518(14), pp.3792-3796. doi: https://doi.org/10.1016/j.tsf.2010.01.003.

Li, Y., Zhang, W., Li, J., Lin, X., Gao, X., Wei, F., Zhang, G. and Li, L., 2021. Microstructure and high temperature mechanical properties of advanced W–3Re alloy reinforced with HfC particles. Materials Science and Engineering: A, 814, p.141198., doi: https://doi.org/10.1016/j.msea.2021.141198.

Liu, J., Zhang, Y., Wang, W., Yang, X., Liu, S., Zhang, J., Guo, Z., Wang, T. and Li, T., 2022. Interfacial enhancement and mechanical properties of CF/Al composites with improved interfacial structure induced by Al–Ni–Mg ternary reaction. Materials Science and Engineering: A, 831, p.142040. doi: https://doi.org/10.1016/j.msea.2021.142040.

Liu, Y., Dan, Y., Bian, Y. and Han, Z., 2019. The thermal conductivity of a composite material with nano-sized nonmetal particles embedded in a metal matrix. Journal of Alloys and Compounds, 801, pp.136-141. doi: https://doi.org/10.1016/j.jallcom.2019 .06.126.

Lloyd, D.J., 1994. Particle reinforced aluminium and magnesium matrix composites. International materials reviews, 39(1), pp.1-23. doi: https://doi.org/10.1179/imr.1994.39.1.1

Lotfpour, M., Bahmani, A., Mirzadeh, H., Emamy, M., Malekan, M., Kim, W.J., Taghizadeh, M. and Afsharnaderi, A., 2021. Effect of microalloying by Ca on the microstructure and mechanical properties of as-cast and wrought Mg–Mg2Si composites. Materials Science and Engineering: A, 820, p.141574. doi: https://doi.org/10.1016/j.msea.2021.141574.

Lv, M., Wang, L., Liu, J., Kong, F., Ling, A., Wang, T. and Wang, Q., 2019. Surface energy, hardness, and tribological properties of carbon-fiber/polytetrafluoroethylene composites modified by proton irradiation. Tribology International, 132, pp.237-243. doi: https://doi.org/10.1016/j.triboint.2018.12.028.

Mazahery, A. and Shabani, M.O., 2013. Microstructural and abrasive wear properties of SiC reinforced aluminum-based composite produced by compocasting. Transactions of Nonferrous Metals Society of China, 23(7), pp.1905-1914. doi: https://doi.org/10.1016/S1003-6326(13)62676-X.

Moheimani, S.K., Keshtgar, A., Khademzadeh, S., Tayebi, M., Rajaee, A. and Saboori, A., 2021. Tribological behaviour of AZ31 magnesium alloy reinforced by bimodal size B4C after precipitation hardening. Journal of Magnesium and Alloys. doi: https://doi.org/10.1016/j.jma.2021.05.016.

Muratov, V.A., Luangvaranunt, T. and Fischer, T.E., 1998. The tribochemistry of silicon nitride: effects of friction, temperature and sliding velocity. Tribology International, 31(10), pp.601-611. doi: https://doi.org/10.1016/S0301-679X(98)00081-4

Ozaki, Y. and Zee, R.H., 1994. High temperature diffusion of hafnium in tungsten and a tungsten-hafnium carbide alloy. Scripta Metallurgica et Materialia;(United States), 30(10). doi: https://doi.org/10.1016/0956-716X(94)90256-9

Paidar, M., Bokov, D., Mehrez, S., Ojo, O.O., Ramalingam, V.V. and Memon, S., 2021. Improvement of mechanical and wear behavior by the development of a new tool for the friction stir processing of Mg/B4C composite. Surface and Coatings Technology, 426, p.127797., doi: https://doi.org/10.1016/j.surfcoat.2021.127797.

Panda, J.N., Bijwe, J. and Pandey, R.K., 2018. Tribo-performance enhancement of PAEK composites using nano/micro-particles of metal chalcogenides. Composites Science and Technology, 167, pp.7-23. doi: https://doi.org/10.1016/j.compscitech.2018.07.014.

Parizi, M.T., Ebrahimi, G.R., Ezatpour, H.R. and Paidar, M., 2019. The structure effect of carbonaceous reinforcement on the microstructural characterization and mechanical behavior of AZ80 magnesium alloy. Journal of Alloys and Compounds, 809, p.151682., doi: https://doi.org/10.1016/j.jallcom.2019.151682.

Poon, C.Y. and Sayles, R.S., 1992. The classification of rough surfce contacts in relation to tribology. Journal of Physics D: Applied Physics, 25(1A), p.A249. doi: https://doi.org/10.1088/0022-3727/25/1A/038

Pramanik, A., 2016. Effects of reinforcement on wear resistance of aluminum matrix composites. Transactions of Nonferrous Metals Society of China, 26(2), pp.348-358. doi: https://doi.org/10.1016/S1003-6326(16)64125-0

Ru, G., Qi, W., Tang, K., Wei, Y. and Xue, T., 2020. Interlayer friction and superlubricity in bilayer graphene and MoS2/MoSe2 van der Waals heterostructures. Tribology International, 151, p.106483. doi: https://doi.org/10.1016/j.triboint.2020.106483

Saeidi, F., Taylor, A.A., Meylan, B., Hoffmann, P. and Wasmer, K., 2017. Origin of scuffing in grey cast iron-steel tribo-system. Materials & Design, 116, pp.622-630. doi: https://doi.org/10.1016/j.matdes.2016.12.044.

Schall, J.D., Gao, G. and Harrison, J.A., 2010. Effects of adhesion and transfer film formation on the tribology of self-mated DLC contacts. The Journal of Physical Chemistry C, 114(12), pp.5321-5330. doi: https://doi.org/10.1021/jp904871t

Singh, H., Kumar, S. and Kumar, D., 2020. The role of in-situ ceramic reinforcements on microstructure evolution and mechanical properties on developed hybrid Mg-MMCs. Materials Science and Engineering: A, 789, p.139577. doi: https://doi.org/10.1016/j.msea.2020.139577

Srivastava, A.K., Nag, A., Dixit, A.R., Scucka, J., Hloch, S., Klichová, D., Hlaváček, P. and Tiwari, S., 2019. Hardness measurement of surfaces on hybrid metal matrix composite created by turning using an abrasive water jet and WED. Measurement, 131, pp.628-639. doi: https://doi.org/10.1016/j.measurement.2018.09.026.

Sumer, M., Unal, H. and Mimaroglu, A., 2008. Evaluation of tribological behaviour of PEEK and glass fibre reinforced PEEK composite under dry sliding and water lubricated conditions. Wear, 265(7-8), pp.1061-1065. doi: https://doi.org/10.1016/j.wear.2008.02.008

Sun, S.K., Zhang, G.J., Liu, J.X., Zou, J. and Ni, D.W., 2013. Reaction sintering of HfC/W cermets with high strength and toughness. Journal of the American Ceramic Society, 96(3), pp.867-872. doi: https://doi.org/10.1111/jace.12139

Swamy, A.R.K., Ramesha, A., Kumar, G.V. and Prakash, J.N., 2011. Effect of particulate reinforcements on the mechanical properties of Al6061-WC and Al6061-Gr MMCs. Journal of minerals and materials characterization and engineering, 10(12), p.1141. doi: 10.4236/jmmce.2011.1012087

Tang, B., Li, H., Guo, N., Zhang, H., Liu, G., Li, X. and Zuo, Y., 2021. Revealing ductile/quasi-cleavage fracture and DRX-affected grain size evolution of AA7075 alloy during hot stamping process. International Journal of Mechanical Sciences, 212, p.106843. doi: https://doi.org/10.1016/j.ijmecsci.2021.106843.

Venkatesh, R. and Rao, V.S., 2018. Thermal, corrosion and wear analysis of copper based metal matrix composites reinforced with alumina and graphite. Defence Technology, 14(4), pp.346-355. doi: https://doi.org/10.1016/j.dt.2018.05.003

Wang, D. and Rong, S., 2021. Study on cast-weld process and composite interface of bimetal composite roll sleeve. Journal of Materials Research and Technology, 12, pp.848-861. doi: https://doi.org/10.1016/j.jmrt.2021.03.032.

Xu, Y., Cartwright, B., Advincula, L., Myant, C. and Stokes, J.R., 2021. Generalised scaling law for soft contact tribology: Influence of load and asymmetric surface deformation. Tribology International, 163, p.107192. doi: https://doi.org/10.1016/j.triboint.2021.107192.

ISSN: 0369-8963

Yamaguchi, E.S., 2003. The importance of progressive techniques in tribology research. Tribology international, 36(10), pp.727-732. doi: https://doi.org/10.1016/S0301-679X(03)00052-5.

Zhang, J., Ma, S., Zhu, J., Kang, K., Luo, G., Wu, C., Shen, Q. and Zhang, L., 2019. Microstructure and compression strength of W/HfC composites synthesized by plasma activated sintering. Metals and Materials International, 25(2), pp.416-424. doi: https://doi.org/10.1007/s12540-018-0190-8

Zhang, L., Luo, X., Liu, J., Leng, Y. and An, L., 2018. Dry sliding wear behavior of Mg-SiC nanocomposites with high volume fractions of reinforcement. Materials Letters, 228, pp.112-115. doi: https://doi.org/10.1016/j.matlet.2018.05.114.

Zhang, Q., Ge, J., Zhang, B., He, C., Wu, Z. and Liang, J., 2022. Effect of thermal residual stress on the tensile properties and damage process of C/SiC composites at high temperatures. Ceramics International, 48(3), pp.3109-3124. doi: https://doi.org/10.1016/j.ceramint.2021.10.085.

Zou, J., Xiao, Q., Chen, B., Li, Y., Han, S., Jiao, Y., Zhang, X., Li, X. and Liang, T., 2021. Effect of HfC addition on the microstructure and properties of W–4.9 Ni–2.1 Fe heavy alloys. Journal of Alloys and Compounds, 872, p.159683., doi: https://doi.org/10.1016/j.jallcom.2021.159683.